OFDMA System Identification using Cyclic Autocorrelation Function: A Software Defined Radio Testbed

Halim Bahadır Tuğrel†, Hakan Alakoca†, Kursat Tekbiyik†, Güneş Karabulut Kurt†, Cem Ayyıldız‡
† Istanbul Technical University, Wireless Communication Research Laboratory (WCRL), Istanbul, Turkey
‡Turkcell Teknoloji Araştırma ve Geliştirme Laboratuvarı, Turkcell İletişim Hizmetleri A.Ş., İstanbul, Türkiye
{tugrel, alakoca, tekbiyik, gkurt}@itu.edu.tr, cem.ayyildiz@gmail.com

***Abstract*—In this paper, cyclic autocorrelation function (CAF) is used for signal type identification. Orthogonal frequency division multiple access (OFDMA) signals with different cyclic prefix lengths are generated by using software defined radio nodes. According to test results, by using the OFDMA frame structure, OFDMA signals are separated from each other, hence signal parameters are differentiated blindly. Additionally, jamming signal and OFDMA signals are distinguished from each other. Real-time measurement results are given to demonstrate the performance of the investigated approach.**

I. Introduction

Wireless communication is one of the fastest growing areas in the engineering world with technological advances. This situation causes high demands by users. Such high demands require high system capacities. System capacity can be extended by increasing the frequency bandwidth. However, it is not easy to acquire new spectrum allocation since electromagnetic spectrum is limited [1]. So, other methods are investigated to improve spectrum efficiency.

One of issues that affect spectrum efficiency is the presence of illegitimate users. Such users can decrease the communication quality, and should be detected and stopped. Hence identifying the transmitted signals and allowing only the transmission of legitimate users is crucial in wireless communication systems.

Received signal identification and detection are required to deal with such problems. With this goal, signal feature extraction has to be applied in order to identify the signal type [2]. After the signal features have been obtained, signal types can be identified by using classifiers [3]. In this work, cyclic autocorrelation function (CAF) is used for identification signal types. OFDM signals, that have different cyclic prefix symbol length, are generated by using Universal Software Radio Peripheral (USRP) 2921 which is one of the software defined radio (SDR). These generated signals are applied the CAF algorithm. Using the own feature parameter of OFDM, signal decomposition was successfully completed according to test result. Also, jamming signal, that is generated USRP 2921, applied to the algorithm. As a result, jamming signal and OFDM signal are separated from each other accurately.

Related Literature

There are several works in the literature focus on the signal type identification. In [4], identification of signal types with different communication protocols is investigated. CAF is used in order to extract the signal features and differentiate between distinct protocols. Besides the simulation results, this algorithm is implemented using USRP2 that is a type of SDR.

In [5], [6], spectral correlation function (SCF), that is the fast fourier transform (FFT) of CAF, is used for spectrum analysis. After extracted signal feature is interpreted, tests have been conducted for more robust and effective system configuration. [7] shows that some important imperfections due to the hardware such as clock and oscillator errors are introduced when cyclostationary analysis for signal feature extraction is implemented. Simulation results are given about cyclic frequency mismatch. SCF is used for cyclostationary analysis as a method.

In [8], SCF RF signal analyzer is demonstrated using USRP software defined radio platform. Estimation of carrier frequency and symbol rate of found signal type is given as a result. [9] aims identification and classification of orthogonal frequency division multiple access (OFDMA) signals. Preamble cross-correlation technique is used in order to detect periodicity between cyclic prefix of the IEEE 802.16e waveform. [10] shows that 16-QAM/OFDM modulated signal is detected using periodicity of pilot subcarriers that are located within the OFDM symbols. SCF is used for cyclostationary signal analysis. In [11], pilot-based, cyclic prefix-based and preamble-based cyclostationary features of Wi-Fi signal are described by using SCF algorithm. [12] demonstrated the localization of interfering signals using CAF cyclostationary feature extraction method.

In [13], cyclostationary feature analysis steps are explained, if there is an interference between different signal types in the same frequency band. In [14], researchers compare multiple energy detection (MED) technique to cyclostationary feature detection technique. According to the simulation results, MED outperforms cyclostationary feature detection technique at -8 dB SNR value.

In this paper, we target to extend the identification problem to the parameters of OFDM signals, mainly targeting the cyclic

prefix (CP) length. Through SDR tests, we capture various signals and differentiate them through their CAF characteristics. Additionally, consistent with the available literature, we also demonstrate the efficacy of jammer identification through the use of CAF.

II. System Model

A. Transmitter Node

Transmitter nodes modulate incoming bits by using 4-QAM symbol mapping. Main transmitter structure of OFDMA signal is given in Fig. 1. Pilot symbols, which are used for channel estimation and synchronization processes, are inserted as 4-QAM modulated signal after the modulation block. $X_{n,l}$ denotes the complex signal assigned to the n^{th} subcarrier of l^{th} OFDMA symbol.

Next, serial data converted to parallel data stream. By using subcarrier allocation block, zero padding inserting operation is handled. $x_{k,l}$ represents the subcarriers in the time domain, and obtained as

$$x_{k,l} = \frac{1}{\sqrt{N}} IFFT\ \left\{X_{n,l}\right\} = \sum_{n=0}^{N-1} X_{n,l}\ e^{\frac{j2\pi kn}{N}}, \qquad (1)$$

at the output of IFFT block. Then CP insertion is handled for protection against multipath channel, while converting back to serialized data from parallel data stream. L symbols of the frame are appended at the beginning of the frame in time domain. Digital OFDMA symbols $s_{k,l}$ are converted to analog waveforms $s_{k,l}(t)$. The transmitted symbol $s_{k,l}$ is modeled as

$$s_{k,l}(t) = \sum_{l=0}^{\infty} x_{k,l}\ \frac{1}{T - T_{CP}}\ e^{j2\pi \frac{w}{N}(t - lT - T_{cp})}, t - lT \in [0, T), \qquad (2)$$

by generating rectangular pulse modulated on carrier frequency kW/N as in [15]. Here, T is referred as total transmission duration and T_{CP} is the transmission duration on CP portion.

B. Jammer Node

A conventional wideband jammer is considered for this system. Its transmission technique mainly depends on OFDM. Let $J_{n,l}$ denote the jamming signal in the frequency domain OFDM symbol of the n^{th} subcarrier of the l^{th} OFDM symbol. Transmitted jamming signal is denoted by $J_{n,l} \sim \mathcal{CN}(0, \sigma_j^2)$, a complex Gaussian distributed random variable with zero mean and σ_j^2 variance. Thus, the signals in the frequency domain is converted to time domain as in OFDM technique and their distribution remains identical, for $k \in \mathcal{N}$ where $\mathcal{N}$ represents the set of subcarriers. The transmitted jammer signals are obtained as

$$j_{k,l} = \frac{1}{\sqrt{N}}\ IFFT\ \left\{J_{n,l}\right\} = \sum_{n=0}^{N-1} j_{n,l}\ e^{\frac{j2\pi kn}{N}}. \qquad (3)$$

C. Receiver Node

Analog received signal are converted to digital signals $r_{k,l}$ by using A/D converter block. Synchronization, a substantial issue in OFDM like systems, is provided by means of CP. The CP portion is removed, i.e. the appended L symbols are removed from the start of the frame. After CP removal, time domain symbols $y_{k,l}$ are converted to a parallel data stream for FFT process. Frequency domain signal $Y_{n,l}$ is expressed as,

$$Y_{n,l} = FFT\ \left\{y_{k,l}\right\} = \frac{1}{\sqrt{N}} \sum_{n=0}^{N-1} y_{k,l}\ e^{-\frac{j2\pi kn}{N}}. \qquad (4)$$

Next, signals are converted to serial data streams. We use least square method fro channel estimation that is mainly dependent on pilot subcarriers. For both configurations, we use one pilot subcarrier for every 8 data subcarriers. Our receiver structure is given in Fig 2. User separation is achieved after the equalizer, by using I/Q separation block, amd performance measurements are realized.

III. Cyclic Autocorrelation Function

The main idea of behind signal feature extraction relies on the observations about wireless protocols. These observations reveal hidden repeated patterns which are necessary and unique for each communication system. For example, Wi-Fi (OFDM PHY) contains CP, which is used in order to prevent intersymbol interference (ISI) and hence to preserve orthogonality between OFDM subcarriers. Also, ZigBee has a repeated pulse, which uses QPSK data transmission. Bluetooth has modulated data bits using FSK that is repeated with a different frequency carrying on the Gaussian pulse. Unique signatures are created for each signal type using these repetitive sequences.

If a signal has a repeated pattern, then if received signal is correlated with delayed version of itself, the result of correlation reaches peaks at periods of repeated pattern. This correlation function is called as cyclic autocorrelation function (CAF) [4].

In our system model, the received signal in time domain, $y_{k,l}$ is used for input of CAF. However, $y_{k,l}$ is reshaped as

$$\mathbf{z} = \begin{bmatrix} y_{1,1} & \cdots & y_{N,1} & \cdots & y_{1,\frac{M}{N}} & \cdots & y_{N,\frac{M}{N}} \end{bmatrix} \qquad (5)$$

$\mathbf{z}$, the array of $y_{k,l}$, is of size $1 \times M$. M represents the total number of received samples. N corresponds to the number of subcarriers in the each OFDMA frame as indicated above. $\frac{M}{N}$ is the total number of OFDMA frames. Then, CAF is obtained as

$$R_z^{\beta}[\tau] = \sum_{m=0}^{M-1} z[m][z^*[m - \tau]]e^{-j2\pi\beta m}, \qquad (6)$$

where $z[m]$ is the m^{th} element of $\mathbf{z}$ for $m \in \{1, 2, \ldots, M\}$. $R_z^{\beta}[\tau]$ reaches a maximum value for suitable τ corresponding to the time period between repeated hidden pattern. Random patterns in $y_{k,l}$ can be exposed to interference. Moreover, obtained peak point values periodically occur in l. Therefore,

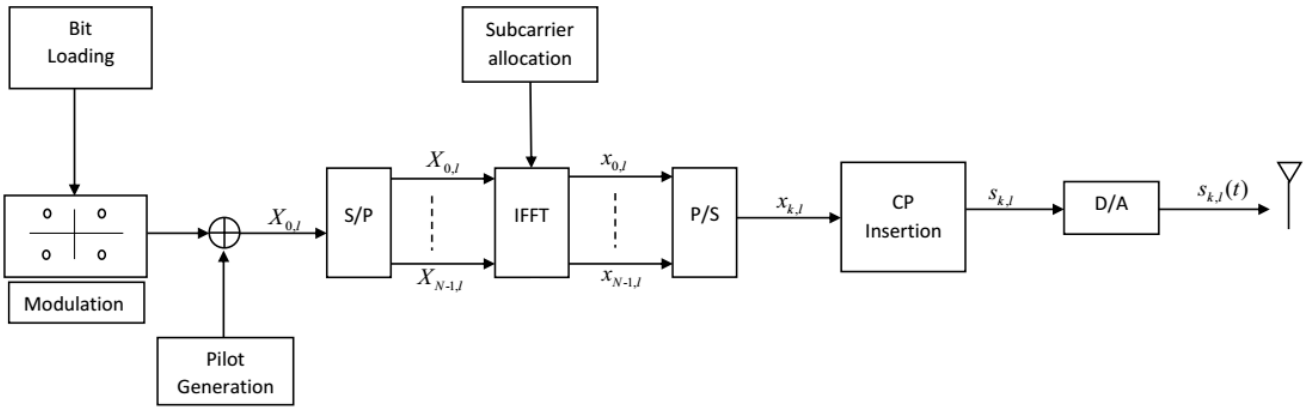

Fig. 1: OFDMA transmitter block diagram.

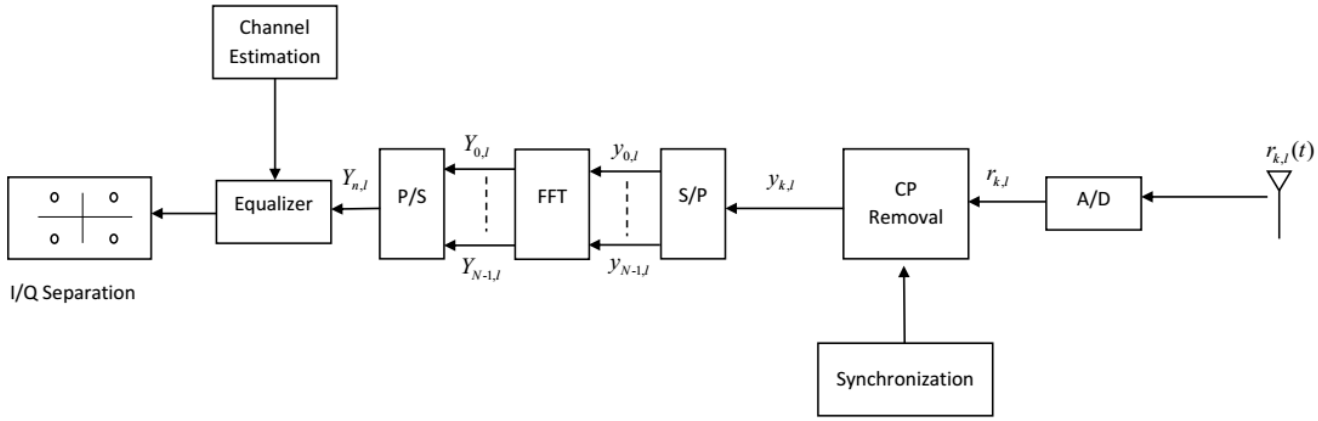

Fig. 2: OFDMA receiver block diagram.

TABLE I: OFDMA frame structure with $N = 128$ subcarriers

Configuration	Zero Padding	Pilot + Information	DC Component	Pilot + Information	Zero Padding
Subcarrier Index	0-27	28-63	64	65-100	101-127
UE-1	28 Subcarriers	36 Subcarriers	1 Subcarrier	36 Subcarriers as ZP	27 Subcarriers
UE-2	28 Subcarriers	36 Subcarriers as ZP	1 Subcarrier	36 Subcarriers	27 Subcarriers

exponential term affects frequency of hidden repeated pattern (β). β can also be called as pattern frequency.

A particular pattern frequency and delay can inform about the signal signatures. For this purpose, Fourier transform of CAF which is called spectral correlation function (SCF) can be used as

$$S_z^{\beta}[f] = \sum_{\tau=-\infty}^{\infty} R_z^{\beta}[\tau] e^{-j2\pi\tau}. \tag{7}$$

If CAF has the peak value at a fixed τ value, SCF has the peak at a specific f value that is inversely proportional to τ, as well. When $R_z^{\beta}[\tau]$ value is placed in (7), we obtain:

$$S_z^{\beta}[f] = \frac{1}{M} \sum_{i=0}^{M-1} Z_{iP}[f][Z_{iP}^{*}[f-\beta]. \tag{8}$$

Here, $Z_{iP}[f]$ is the FFT of received signal ($z[m]$) for the i^{th} time window with length P. x^* represents the complex conjugate of x. Finally, M, that can be defined in the another way, is the total number of successively retrieved time windows of received signal.

IV. Testbed Properties

Our real time measurement setup consists of three nodes; two NI USRP 2921 nodes acting as transmitter and a NI

TABLE II: OFDMA frame structure with $N = 256$ subcarriers

Configuration	Zero Padding	Pilot + Information	DC Component	Pilot + Information	Zero Padding
Subcarrier Index	0-55	56-128	129	130-201	202-255
UE-1	56 Subcarriers	72 Subcarriers	1 Subcarrier	72 Subcarriers as ZP	55 Subcarriers
UE-2	56 Subcarriers	72 Subcarriers as ZP	1 Subcarrier	72 Subcarriers	55 Subcarriers

PXI 1082 node acting as receiver. NI USRP 2921 nodes that are used as transmitter node, can operate in the 2.4-2.5 and 4.9-5.9 GHz frequency bands. We use NI PXI 1082 as receiver node, which includes RFSA module for signal analyses. Implementation is completed according to the system model. All nodes are programmed with NI-LabVIEW, a visual programming language that is used for system designing.

Synchronization, a challenge for OFDM based systems, is provided by both hardware and software solutions. On the hardware side, NI-PXI 6683 timing and synchronization module is used as the 10 MHz clock signal source. On the software side, synchronization is achieved by both NI-RFSG signal and clocking generation software and NI-LabVIEW for controlling generated clocking signals. Additionally, time and frequency offset algorithm in [16] is implemented in the receiver node for improving synchronization accuracy. Hardware components and testbed environment are shown in Fig. 3. We also note that, distance between antenna of NI-PXI 1082 OFDMA receiver and OFDMA User-1 is 40 cm, thus distance between antenna of NI-PXI 1082 OFDMA receiver and OFDMA User-2 is 20 cm for asymmetric data transmission.

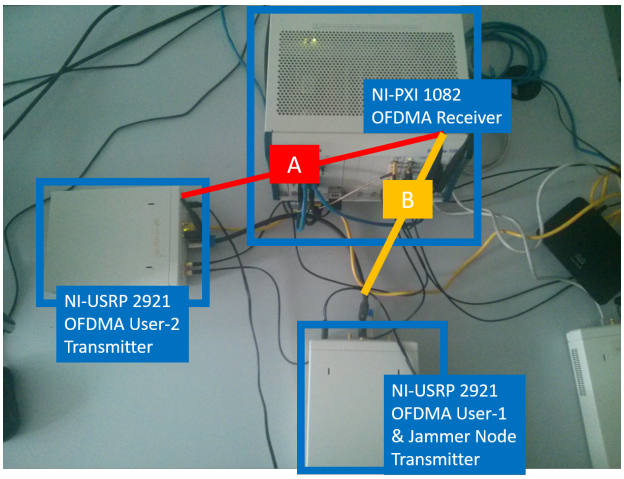

Fig. 3: NI USRP 2921 nodes are used for both OFDMA transmitter nodes and jammer node. NI PXI 1082 module is used for receiver node, clocking and synchronization. For asymmetric transmission distance A is adjusted 40 cm and distance B is 20 cm.

A. *Transmitter Nodes*

OFDMA transmitter nodes are implemented according to our system parameters given in Table I and Table II for $N = 128$ and $N = 256$, respectively. Also, PHY properties of OFDMA based system measurements with N=128 subcarriers is shown in Table III Measurement parameters are configured by means of USRP configuration Virtual Instruments (VIs), which provides the coordination between hardware and software. 72 bits are loaded into the system to generate 4-QAM symbols for $N = 128$ subcarrier OFDMA system. For $N = 256$ subcarriers 128 bits are generated for bit loading operation. Pilot symbols are generated with pseudonoise sequence and also modulated by using 4-QAM symbols. Pilot symbols and subcarrier distribution functions are generated by means of array functions in LabVIEW. Also, we use zero padding for guard subcarrier as 56 subcarriers for $N = 128$ and 112 subcarriers for $N = 256$ based model. CP lengths are set to different values for system identification.

B. *Jammer Node*

Jammer node is configured by using USRP configuration VIs, as in the case of transmitter nodes. Jamming signal transmitter is operating on 2.45 GHz carrier frequency with 1 MS/s I/Q rate. Attack symbols are randomly generated by using Additive White Gaussian Noise VI. Output power is scaled corresponding to non-zero subcarriers of information symbols.

TABLE III: PHY properties of OFDMA based system measurements for both two configuration

System Parameters	Config - I	Config - II
Carrier frequency	2.45 GHz	2.45 GHz
I/Q data rate	1 MS/sec	1 MS/sec
Transmission Bandwidth	1.25 MHz	2.50 MHz
Number of bits used in one frame	72 bits	128 bits
Number of 4-QAM symbols	36 subcarrier	72 subcarrier
Number of pilot subcarrier	4	8
Number of information subcarrier	32	64
Zero padding length (including DC)	56	112
IFFT/FFT length (N)	128	256

C. Receiver Node

OFDMA receiver node is configured by using RFSA configuration VIs, operating with 1 MS/s at 2.45 GHz carrier frequency. All receiver functionalities described in the system model are included in the receiver node. CP removal, zero padding removal, pilot and data decomposition operations are performed by using array functions. Also, linear interpolation based channel estimation and zero forcing equalization are used. I/Q data of complete measurements and performance monitoring results are logged at the receiver node.

V. Measurement Results

A. Received Node Measurements

We first present OFDMA received signal for both user's transmit data. Both two user's data successfully separated from each other at the receiver node, thus received constellation diagrams are given in Fig. 4 for both two users corresponding to both $N = 128$ and $N = 256$ subcarriers.

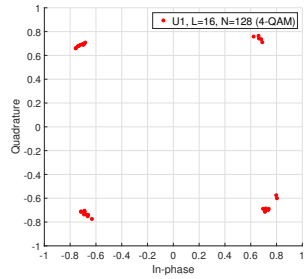

(a) User-1 received signals with N=128 and L=16

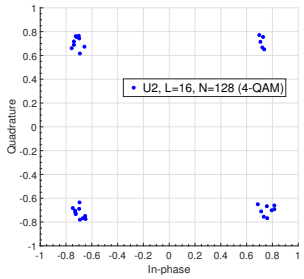

(b) User-2 received signals with N=128 and L=16

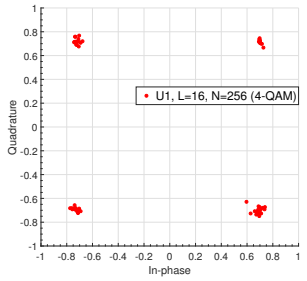

(c) User-1 received signals with N=256 and L=16

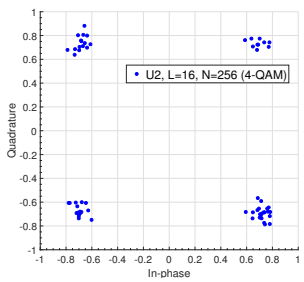

(d) User-2 received signals with N=256 and L=16

Fig. 4: Constellation diagrams for both two different configuration and both two user case

CP is used for fixing of time and frequency offset and protection against multipath channel delay spread. CP length, L is varied. Fig. 5 depicts the EVM performance of both users according to different CP lengths. OFDMA transmission is sensitive to CP length both users, thus performance degradation occurs up to a threshold value. Exceeding $L = 32$ as the CP length, the received signal deteriorates the EVM performance both users. For instance considering User-1 EVM measurement is increased by 430.72%, while switching L value from $L = 32$ to $L = 64$. As inequality of the distance of user's transmitter node and receiver node, received signals are considerably different from each other in terms of EVM performance.

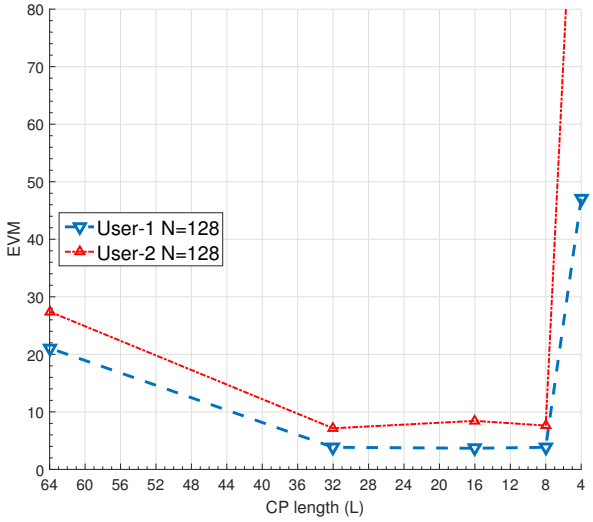

Fig. 5: EVM performance against CP length (L)

Received signal FFT measurements of both configuration considering decreasing CP length from $L = 16$ to $L = 4$ is given in Fig. 6. As indicated before, because of asymmetric transmission amplitudes of signals, the data transmission performances are different from each other for both user configurations. Received signal deterioration which is experimentally observed with decreasing CP length (as $L = 4$), is effected by multipath channel delay spread for both cases.

B. CAF of OFDMA Signals Measurements

As above-mentioned, OFDMA signals, which have the hidden repeated patterns, were used as an input to CAF calculation algorithm. Although OFDMA signals have the same communication protocol, these signals were separated from each other by using their own features of OFDMA signals like CPs with varying lengths. CAF results of OFDMA signals with different CP length can be obtained depending on time delay (τ) and pattern frequency (β). Result of CAF algorithm and normalized CAF algorithm are shown at constant lag of time for OFDMA signal that has different CP symbol lengths at user 1 with 128 subcarriers in Fig. 7 and Fig. 8, respectively. According to the test results, when CP length is increased in the result of CAF, the peak value becomes sharper than smaller CP length. Moreover, when CP length is increased, the beamwidth of the main lobe of CAF varies.

C. CAF of Jamming Signal Measurements

Additionally, jamming signal and OFDMA signal with different CP length are distinguished from each other by using CAF result. The main idea of this separation is that OFDMA signal and jamming signal have different communication protocol types. In Fig. 9, result of normalized CAF algorithm is

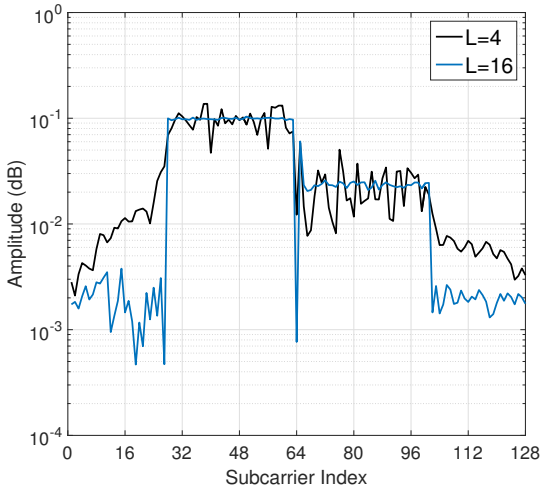

(a) Effect of different CP length on in N=128 point FFT

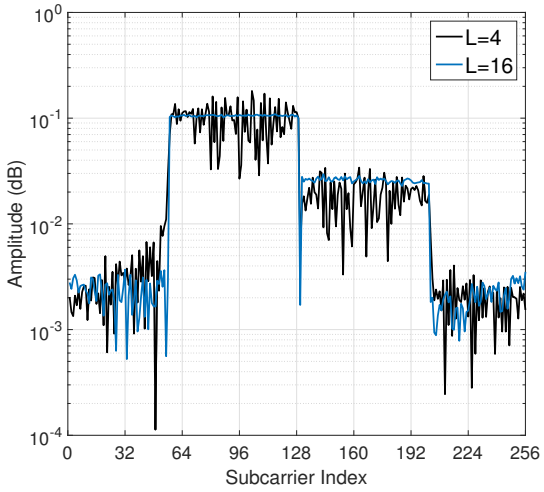

(b) Effect of different CP length on in N=256 point FFT

Fig. 6: Received signal amplitude corresponding to subcarrier index for both two configurations with different CP lengths.

shown at a constant lag of time for jamming signal and OFDM signal at user 1 with 128 subcarriers. According to CAF results of jamming and OFDMA signals, these signals can be easily separated from each other.

Besides CAF results, SCF results were used in order to show differences between OFDMA signals and jamming signals. SCF is more efficient and robust than CAF in hardware applications, because signal processing in the frequency domain is less complex than signal processing in the time domain. In Fig. 10, result of SCF algorithm is shown at constant lag of time for OFDM signal that with $L = 64$ and $N = 256$ for user 1. In Fig. 11, result of SCF algorithm is shown constant lag of time for jamming signal with 256 subcarriers.

According to SCF results of jamming and OFDMA signals, we can observe that these signals can be accurately distinguished from each other. In addition to this, SCF of jamming

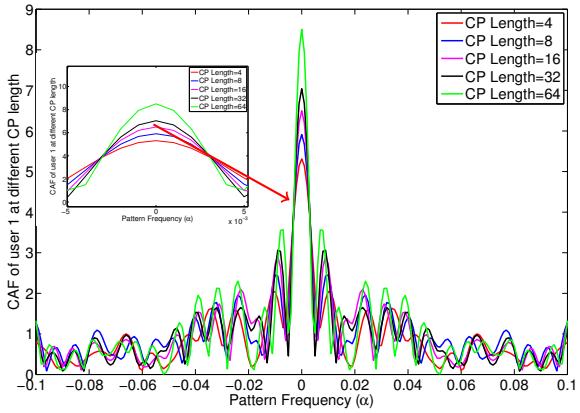

Fig. 7: CAF of user 1 at different CP length and constant lag of time (τ) for 128 subcarriers OFDM

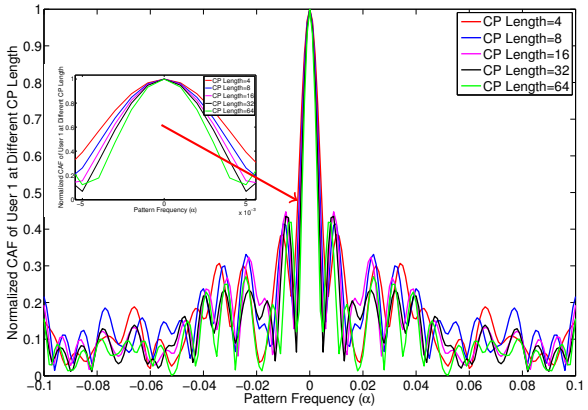

Fig. 8: Normalized CAF of user 1 at different CP length and constant lag of time (τ) for 128 subcarriers OFDM

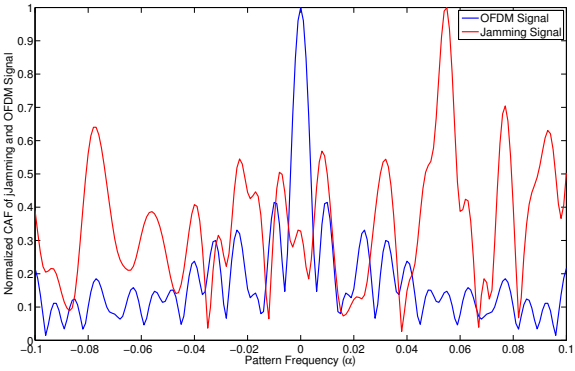

Fig. 9: Normalized CAF of jamming signal and OFDM signal, which has $L = 8$, at constant lag of time (τ) for $N = 128$.

signal behaves like a noise, in line with theoretical results [17].

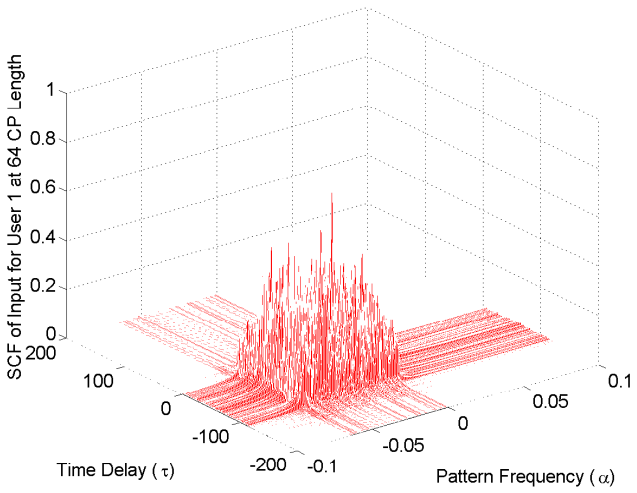

Fig. 10: SCF of User 1 for $L = 64$ and $N = 256$.

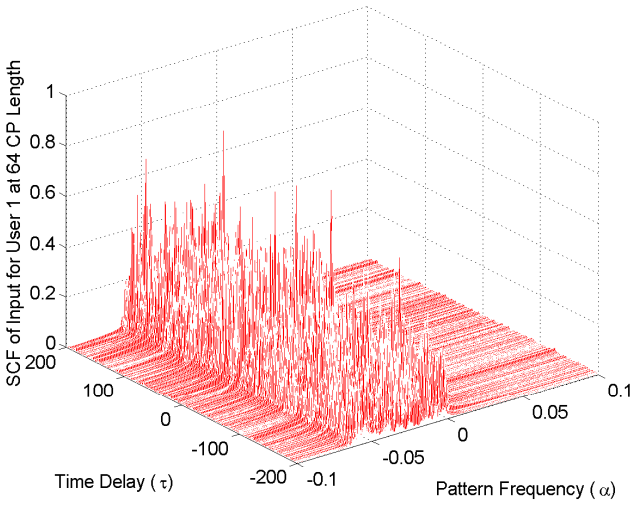

Fig. 11: SCF of Jamming Signal.

VI. Conclusion

This paper discusses postprocess results of CAF and SCF based identification technique of OFDMA and jamming signals generated from USRP 2921 based testbed. From test results we deduce two main observations. Firstly, generated OFDMA and jamming signals can be separated from each other by using CAF. Feature vectors of these two signal types are clearly different from each other because of the hidden repeated patterns. Secondly, the periodicity of cyclic prefix is used in order to extract the feature (CP length) of OFDMA signals. This extracted feature vector of OFDMA signals are useful in order to distinguish itself from other type of signals. Furthermore, the CP lengths of OFDMA signals can be differentiated through CAF tests.

As future work, an SVM classifier will be designed for a more detailed classification. Furthermore, other communication protocols will be added for signal identification in the ISM band such as Bluetooth and ZigBee.

References

[1] K. Po and J.-i. Takada, "Signal detection method based on cyclostationarity for cognitive radio," *The Institute of Electronics, Information and Communication Engineers, Technical Report of IEICE*, 2007.

[2] V. Šebesta, R. Maršálek, and Z. Fedra, "OFDM signal detector based on cyclic autocorrelation function and its properties," *Radioengineering*, vol. 20, no. 4, p. 927, 2011.

[3] Z. Xin, W. Ying, and Y. Bin, "Signal classification method based on support vector machine and high-order cumulants," *Wireless Sensor Network*, vol. 2, no. 01, p. 48, 2010.

[4] S. S. Hong and S. R. Katti, "DOF: a local wireless information plane," in *ACM SIGCOMM Computer Communication Review*, vol. 41, no. 4. ACM, 2011, pp. 230–241.

[5] J. Chen, A. Gibson, and J. Zafar, "Cyclostationary spectrum detection in cognitive radios," in *IET Seminar on Cognitive Radio and Software Defined Radios: Technologies and Techniques*. IET, 2008, pp. 1–5.

[6] P. D. Sutton, K. E. Nolan, and L. E. Doyle, "Cyclostationary signatures in practical cognitive radio applications," *IEEE Journal on selected areas in Communications*, vol. 26, no. 1, pp. 13–24, 2008.

[7] Y. Zeng and Y.-C. Liang, "Robustness of the cyclostationary detection to cyclic frequency mismatch," in *21st Annual IEEE International Symposium on Personal, Indoor and Mobile Radio Communications*, 2010, pp. 2704–2709.

[8] R. Zhou, X. Li, T. Yang, Z. Liu, and Z. Wu, "Real-time cyclostationary analysis for cognitive radio via software defined radio," in *IEEE Global Communications Conference (GLOBECOM)*, 2012, pp. 1495–1500.

[9] R. Gray, M. Tummala, J. McEachen, J. Scrofani, and D. Garren, "Identification and classification of Orthogonal Frequency Division Multiple Access signals," in *IEEE 6th International Conference on Signal Processing and Communication Systems (ICSPCS)*, 2012, pp. 1–6.

[10] A. A. Thomas and T. Sudha, "Primary user signal detection in cognitive radio networks using cyclostationary feature analysis," in *IEEE National Conference on Communication, Signal Processing and Networking (NCCSN)*, 2014, pp. 1–5.

[11] C. Du, H. Zeng, W. Lou, and Y. T. Hou, "On cyclostationary analysis of WiFi signals for direction estimation," in *IEEE International Conference on Communications (ICC)*. IEEE, 2015, pp. 3557–3561.

[12] K. Joshi, S. Hong, and S. Katti, "Pinpoint: Localizing interfering radios," in *Presented as part of the 10th USENIX Symposium on Networked Systems Design and Implementation (NSDI 13)*, 2013, pp. 241–253.

[13] Q. Yuan, P. Tao, W. Wenbo, and Q. Rongrong, "Cyclostationarity-based spectrum sensing for wideband cognitive radio," in *IEEE International Conference on Communications and Mobile Computing*, vol. 1, 2009, pp. 107–111.

[14] A. Bagwari and G. S. Tomar, "Multiple energy detection Vs cyclostationary feature detection spectrum sensing technique," in *IEEE 4th International Conference on Communication Systems and Network Technologies (CSNT)*, 2014, pp. 178–181.

[15] O. Edfors, M. Sandell, J.-J. van de Beek, D. Landström, and F. Sjöberg, "An introduction to orthogonal frequency-division multiplexing," *Div. of Signal Processing, Research Report*, 1996.

[16] J.-J. Van de Beek, M. Sandell, P. O. Borjesson *et al.*, "ML estimation of time and frequency offset in OFDM systems," *IEEE transactions on signal processing*, vol. 45, no. 7, pp. 1800–1805, 1997.

[17] R. F. Ústok *et al.*, "Spectrum sensing based on cyclostationary feature detection for cognitive radios with multiple antennas," in *2011 IEEE 19th Signal Processing and Communications Applications Conference (SIU)*. IEEE, 2011, pp. 550–553.